



**HAL**  
open science

# 1.5 $\mu$ m Lidar anemometer for True Air Speed, Angle Of Sideslip and Angle Of Attack measurements onboard Piaggio P180 aircraft

B. Augère, B. Besson, D. Fleury, D. Goular, C. Planchat, M. Valla

► **To cite this version:**

B. Augère, B. Besson, D. Fleury, D. Goular, C. Planchat, et al.. 1.5 $\mu$ m Lidar anemometer for True Air Speed, Angle Of Sideslip and Angle Of Attack measurements onboard Piaggio P180 aircraft. Measurement Science and Technology, 2016, 27 (5), 10.1088/0957-0233/27/5/054002 . hal-01111306

**HAL Id: hal-01111306**

**<https://hal.science/hal-01111306>**

Submitted on 2 Feb 2015

**HAL** is a multi-disciplinary open access archive for the deposit and dissemination of scientific research documents, whether they are published or not. The documents may come from teaching and research institutions in France or abroad, or from public or private research centers.

L'archive ouverte pluridisciplinaire **HAL**, est destinée au dépôt et à la diffusion de documents scientifiques de niveau recherche, publiés ou non, émanant des établissements d'enseignement et de recherche français ou étrangers, des laboratoires publics ou privés.



Distributed under a Creative Commons Attribution - NonCommercial 4.0 International License

**Title:** 1.5 $\mu$ m Lidar anemometer for True Air Speed, Angle Of Sideslip and Angle Of Attack measurements onboard Piaggio P180 aircraft.

**Society:**

Office National d'Etudes et de Recherches Aérospatiales (ONERA),  
Département d'Optique Théorique et Appliquées (DOTA), BP 80100, 91123 Palaiseau cedex,  
France

**Authors:** B. Augere, B. Besson, D. Fleury, D. Goular, C. Planchat, M.Valla

**Abstract:**

Lidar (Light detection and ranging) is a well established measurement method for the prediction of atmospheric motions through velocity measurements. Recent advances in 1.5 $\mu$ m Lidars show that the technology is mature, offers great ease of use and is reliable and compact. A 1.5 $\mu$ m airborne Lidar appears to be a good candidate for airborne in-flight measurement systems: it allows to measure remotely, outside aircraft aerodynamic disturbance, an absolute air speed (no need of calibration) with a great precision and in all aircraft flight domain.

In the frame work of the EU AIM2 project, Onera task has consisted in the development and testing of a 1.5 $\mu$ m anemometer sensor for in-flight airspeed measurements. Objective of this work is to demonstrate that the 1.5 $\mu$ m Lidar sensor can increase the quality of the data acquisition procedure for the aircraft flight test certification.

This paper presents the 1.5 $\mu$ m anemometer sensor dedicated to in-flight airspeed measurements and describes the flight tests performed successfully onboard the Piaggio P180 aircraft. Lidar air data have been graphically compared to the air data provided by the aircraft Flight Test Instrumentation (FTI) in the reference frame of the Lidar sensor head. Very good agreement of True Air Speed (TAS), Angle Of Sideslip (AOS) and Angle Of Attack (AOA) was observed.

**Keywords**

Lidar, anemometer, 1.5 $\mu$ m technology, in-flight, Piaggio aircraft

## 1. Introduction

Calibration of air data sensor of aircraft requires cumbersome procedures including specific equipment and dedicated flight tests. Such calibration flight tests are often long and costly. Although several techniques have been developed over the years, the most direct and probably the most accurate way to directly obtain the correction factors is to compare the aircraft air data measurements with optically derived measurements obtained non-intrusively from the free stream region in front of the aircraft. Calibrations of the pitot static system and vanes using a laser anemometer have an increased accuracy compared with those obtained with conventional techniques, such as using a towed cone, tower-fly-by, or a pacer aircraft [1]. Laser anemometer allows a precise and remote measurement of air speed, derived from light scattering, just outside the range of the flow disturbance from the aircraft: it is able to give the velocity in real time with no in-flight calibration using autonomous onboard equipment and without a priori assumptions on the atmosphere.

Due to recent progress in fibre lasers and amplifiers, 1.5 $\mu\text{m}$  fibre Lidar technology is becoming a serious candidate for lightweight, compact, eye safe airborne anemometer probes [2]. Such anemometer probes for true air speed measurements with high velocity precision have already been flight tested [3], [4]. In 2003, DALHEC, a 3 axes wind Lidar was built and flown on board a Dauphin helicopter [5]. It was dedicated to True Air Speed measurements at medium range (30-100 m), away from rotor flow perturbations. The volume of the optical head was 1 litre, the processing rack around 200 litres. The original architecture has brought consistent progress in all fibre Lidar technology. This device has been flight tested up to 9000ft altitude.

The 1.5  $\mu\text{m}$  Lidar presented in this paper has been developed in the framework of the European project AIM2 which aims at developing powerful and airborne techniques to reduce duration and cost of flight tests. Its design is based on the latest fiber components commercially available today.

This paper describes the design, manufacture and test of the 1.5 $\mu\text{m}$  anemometer Lidar sensor for in-flight airspeed measurement on Piaggio P180 aircraft. The objective was to demonstrate that airspeed measurement by Lidar technique enhances the quality of the data acquisition process during flight test certification [6], [7].

## 2. Lidar anemometer description

### 1.1 Lidar anemometer functional presentation

Lidar technique measurement is based on Doppler shift determination of a light wave obtained from a single frequency laser that is reflected on natural atmospheric aerosols (Mie scattering). The aerosols are the wind field tracers to be analysed. The frequency shift is proportional to the air velocity and is detected via an interferometer measuring the beat frequency between the backscattered wave from aerosols and a reference wave (local oscillator). Coherent mixing enables the recovery of the backscattered wave phase. This phase contains the radial velocity information (along the laser line of sight). It also enhances the detection sensitivity thanks to the optical product of the signal beam with the reference beam which enables small target signal amplification. If required, the true air speed in three axes can be derived from multi axes sensing. This can be performed using 3 beams or more or a scanning device [8].

Lidar capability to measure True Air Speed (TAS), Angle Of Sideslip (AOS) and Angle Of Attack (AOA)) should meet the following operational requirements for certification process:

- TAS dynamic:  $50\text{m/s} \leq V_x \leq 200\text{m/s}$
- TAS accuracy:  $\leq 1\text{m/s}$
- Angle dynamic:  $-20^\circ \leq \text{AOS} \leq +20^\circ$  ;  $-2^\circ \leq \text{AOA} \leq +15^\circ$
- Angle accuracy:  $0.5^\circ$
- Measurement frequency: 16 Hz.

The Lidar sensor measures the aircraft true air speed projected on its laser axes. A Lidar configuration with 4 axes is chosen to access dynamic evaluation of the True Air Speed (TAS) vector, the angle of Sideslip (AOS) and the Angle Of Attack (AOA) in maneuver and to provide measurements reliability due to redundancy of the fourth axis: The 4 Lidar axes are time multiplexed by a fiber optical switch.

By switching the laser beam along 4 different directions (Figure 1), the Lidar system measures 4 airspeed components respectively  $V_1$ ,  $V_2$ ,  $V_3$  and  $V_4$ . The laser axes are chosen to obtain the 3 components of speed vector  $V_x$ ,  $V_y$  and  $V_z$  in the Sensor Head reference frame (close to aircraft frame) so as to fulfill accuracy and measurement dynamics requirements. The 3 components of the speed vector are derived using a least square approach:

$$\begin{bmatrix} V_x \\ V_y \\ V_z \end{bmatrix} = (M^t M)^{-1} M^t \begin{bmatrix} V_1 \\ V_2 \\ V_3 \\ V_4 \end{bmatrix} \quad M = \begin{bmatrix} \sin \theta \cos \alpha_1 & \cos \theta \cos \alpha_1 & \sin \alpha_1 \\ \sin \theta \cos \alpha_2 & \cos \theta \cos \alpha_2 & \sin \alpha_2 \\ -\sin \theta \cos \alpha_3 & \cos \theta \cos \alpha_3 & \sin \alpha_3 \\ -\sin \theta \cos \alpha_4 & \cos \theta \cos \alpha_4 & \sin \alpha_4 \end{bmatrix}$$

Angles are chosen:

- To minimize airspeed error (more angle is open, there is less error)
- To allow a measurement in an homogenous volume
- To respect the dynamics of the Lidar measurement

These considerations lead to the choice of the following values:

$$\alpha_1 = 45^\circ, \alpha_2 = 0^\circ, \alpha_3 = 40^\circ, \alpha_4 = -5^\circ; \theta = 25^\circ$$

$\Rightarrow$  The error on airspeed vector components is dependent on the error per axis (noted stdaxis), and is equal to:  $\text{std}V_x = 1,35 \text{ stdaxis}$ ,  $\text{std}V_y = 0,75 \text{ stdaxis}$   $\text{std}V_z = 1,25 \text{ stdaxis}$

The larger error is given by the airspeed component  $V_x$  which yields a requirement on the precision equal to 0.2m/s and a maximal precision per axis of  $\text{stdaxis}=0.15\text{m/s}$ .

$\Rightarrow$  AOA, AOS are then deduced from full air speed vector with a good precision inferior of  $0.5^\circ$ :

$$\text{AOA} = \tan^{-1}(V_z/V_x) \quad \text{AOS} = \tan^{-1}\left(V_y / \sqrt{V_x^2 + V_z^2}\right)$$

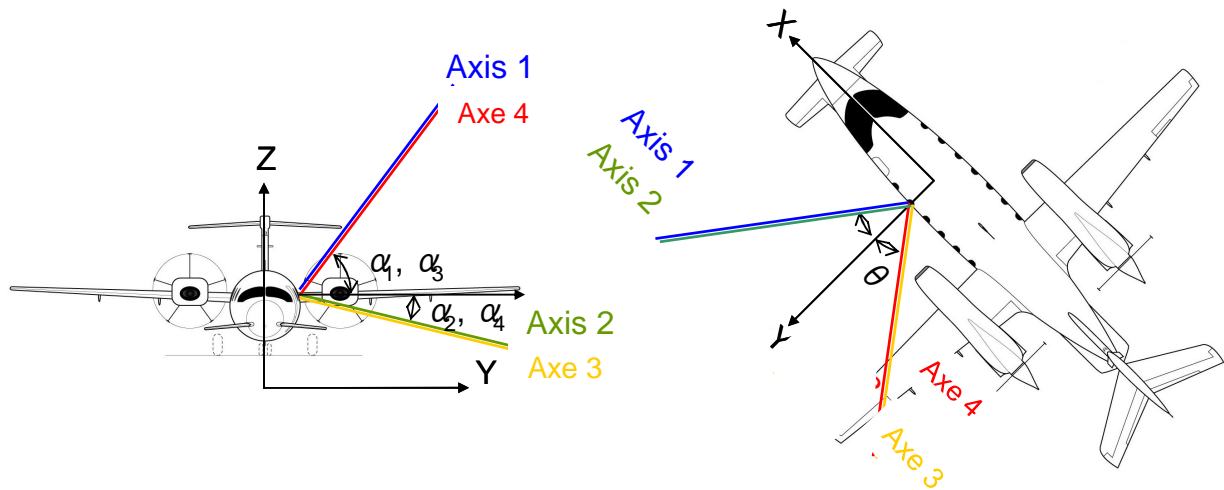


Figure 1: Definition of axes geometry.

## 1.2 Lidar anemometer design and build

1.5  $\mu\text{m}$  technology is the baseline design because of the breakthrough of Erbium doped fiber lasers. In fact, fiber lasers are compact and deliver an eye safe beam with a narrow spectrum and spatial features adapted to coherent anemometry. Moreover, the 1.5  $\mu\text{m}$  radiation draws benefit from the telecommunications technological developments: it allows the design of reliable and compact fiber optical architectures and uses low noise fast detectors and efficient fiber components. Other advantages can be obtained from the use of optical fibers: firstly, it enables the separation of the sensor optical head from electronics and signal processing hardware; secondly it enables to simplify the implementation and the cost because the system adjustments are easier. The Lidar dedicated to in-flight tests is an all fiber system built with of the shelf components.

Lidar implementation in aircraft was studied using CATIA models of the P180 cabin provided by Piaggio. The first cabin window on the left side of the aircraft was modified to insert a glass window suited to the 4 axes Lidar emission. The general structure of the Lidar and its implementation in the aircraft are illustrated on Figure 2.

- ✓ The driving unit composed of 4 racks which are compatible with aeronautic constrains (laser rack, optical/electronic detection rack, power rack and PC rack) and are located in a bay provided by Piaggio.
- ✓ The Sensor head which is precisely positioned with respect to the aircraft reference frame. The 4 Lidar beams are sent through an optical grade glass window to probe the atmosphere and measure the true air speed.

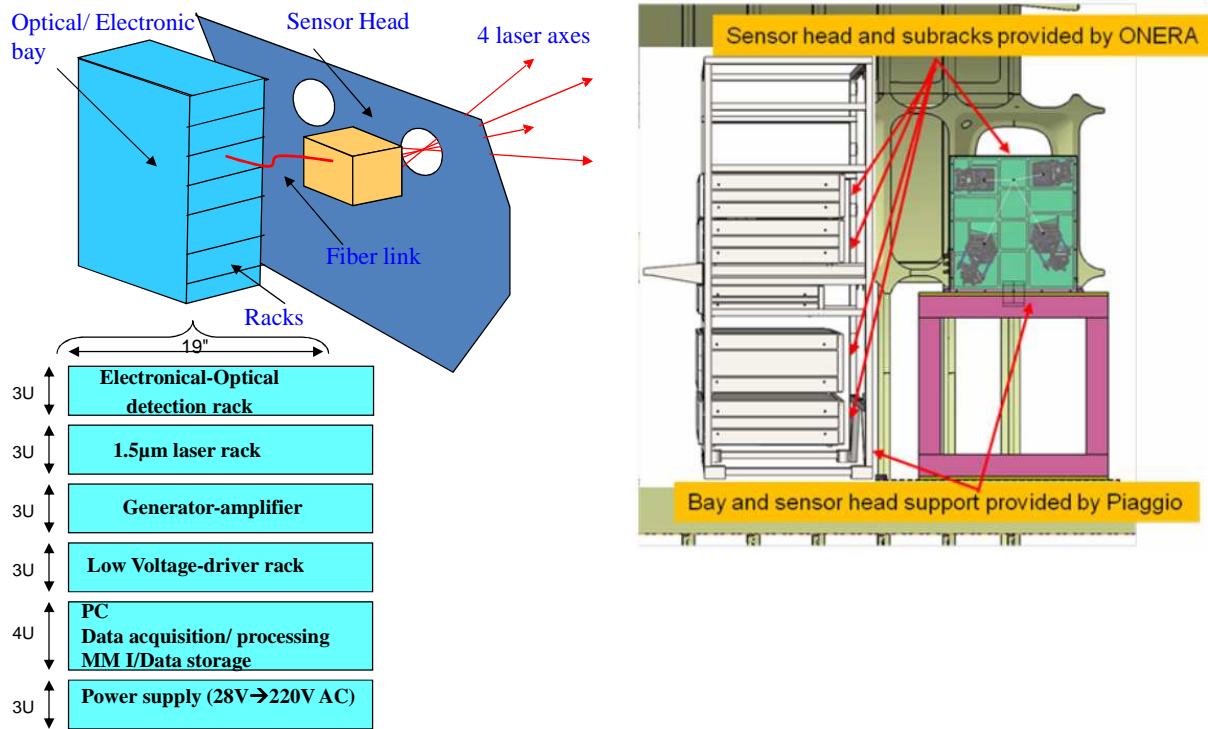


Figure 2: Lidar general description

The Lidar sensor has been designed to meet the flight test requirements in term of airspeed measurement (data rate, TAS precision) and in term of aircraft installation constraints. Figure 3 shows the Lidar anemometer system.

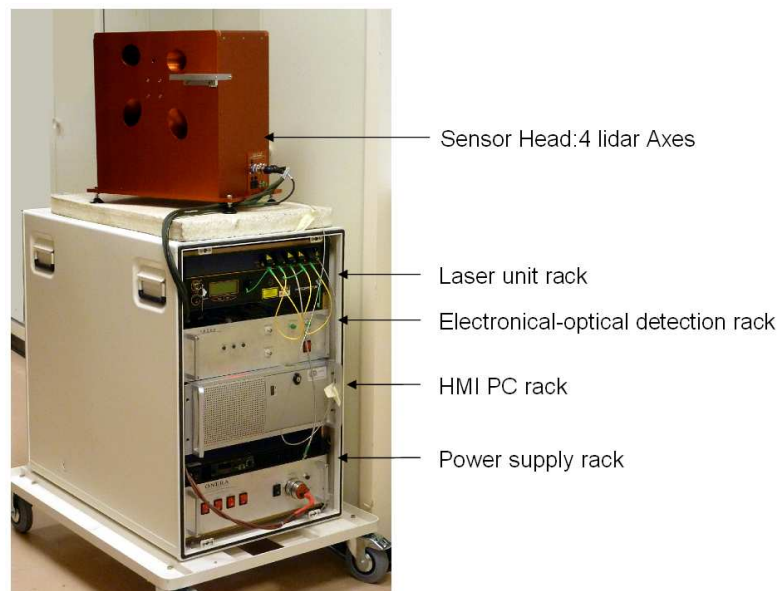


Figure 3: AIM2 Lidar system

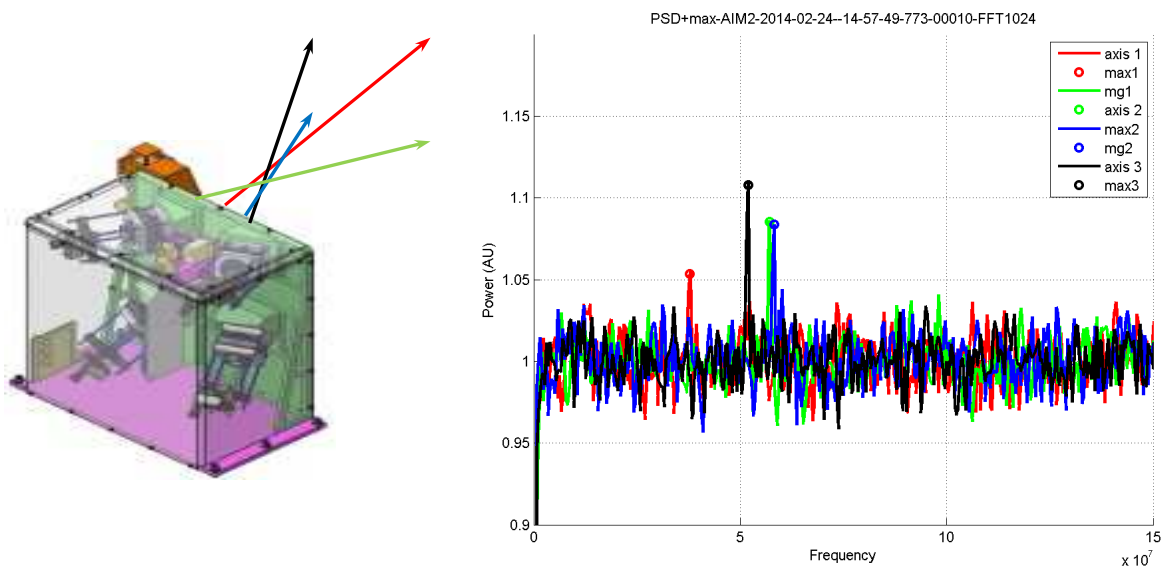
### 3 LIDAR flight tests on board the P180 Prototype

#### 3.1 Lidar Flight tests description

Lidar anemometer has to be evaluated in flight as a reference system to perform air data calibration. The Lidar sensor will be able to measure the aircraft true airspeed (TAS) and tests procedures have been defined by Piaggio so as to infer static error, AOS and AOA. During all tests, air data from the previously calibrated aircraft boom were recorded for flight data analysis and comparison with the Lidar data.

#### 3.2 Description of Lidar signal processing

The first step of signal processing focuses on temporal data sequentially acquired from the four beams of the Lidar. A power spectral density is computed every  $2.6\mu\text{s}$  and to improve the signal to noise ratio each spectrum is averaged using 13ms of signal acquired on each Lidar axis. Figure 4 on the right handside shows an example of the recorded four averaged spectra (colour codes corresponding to the Lidar axes are shown on the left handside). An averaged spectrum consists in a white noise floor and a signal peak. The Doppler frequency shift (proportional to the radial wind speed) is estimated from each Lidar axis averaged spectrum.



Sensor head with 4 Doppler measurement axes

Power Spectral Density for each axis and maximum detection

Figure 4: Recordings of power spectral densities

The output of the signal processing second step are the four Doppler frequencies (or the radial wind speeds), computed every 100 ms in order to take into account the time required to switch from an axis to another. Time series are displayed on Figure 5.

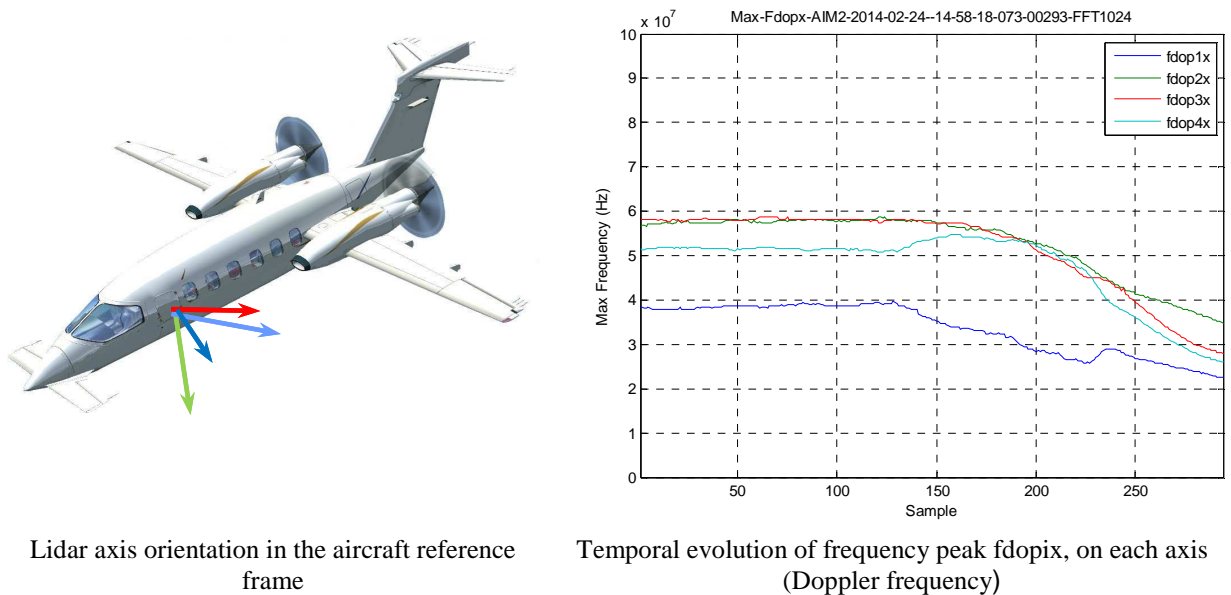


Figure 5: Doppler frequencies time series.

The final step of signal processing is to convert the Lidar radial wind speeds into a 3D air speed vector in the aircraft reference frame, as shown on Figure 6 right (beams colour code is on the left handside).

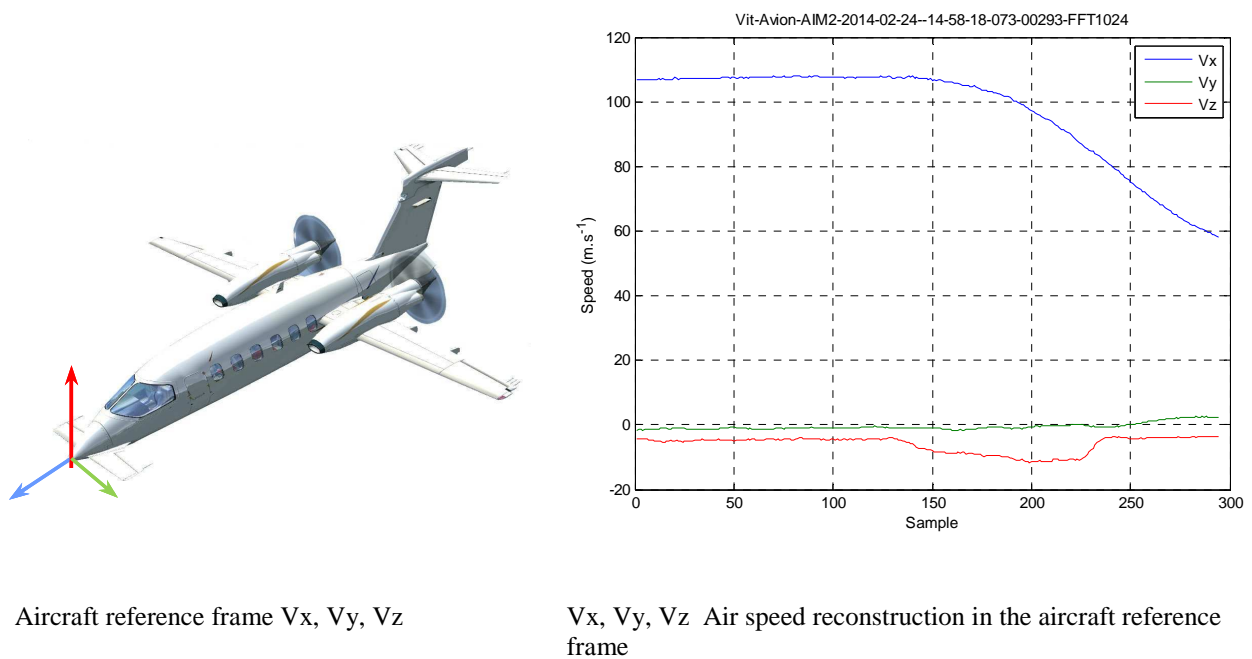


Figure 6: Reconstruction of the airspeed components.



### 1.3 Lidar installation and adjustment onboard P180

Figure 7 presents the Lidar installation on board P180. The glass window integrated by Piaggio in the first cabin window has been chosen for its optical qualities (planarity, transmission), size and thickness compatibles with aeronautic and Lidar constrains.



Figure 7 : Lidar anemometer installation on board P180.

The Sensor head orientation must be known with an accuracy better than  $0.5^\circ$  in the aircraft reference frame in order to meet the AOA and AOS accuracy requirements: its position has been adjusted in terms of distance and alignment and horizontality of the sensor head has been checked using specific procedures.

### 1.4 Lidar anemometer flight tests results

Results presented in this chapter are an illustration of Lidar data measured during steady flight tests and dynamic flight tests allowing comparison between Lidar and Flight Test Instrumentation (FTI). It should be noted that up to now this comparison is graphical, and reconstruction is done in the reference frame of the Lidar. The graphical comparison is based on 6 graphics for each test:

- The top left figure shows the radial wind speed on each Lidar axes.
- The top center figure shows the 3 components of wind speed measured by the Lidar.
- The top right figure shows the altitude given by FTI.
- The 3 bottom figures compare Lidar data (red) and FTI data (blue & green) for TAS, AOA and AOS.

## Accuracy checks of the LIDAR

- LIDAR anemometer results in accuracy check: Multiple ground tracks for airspeed error.

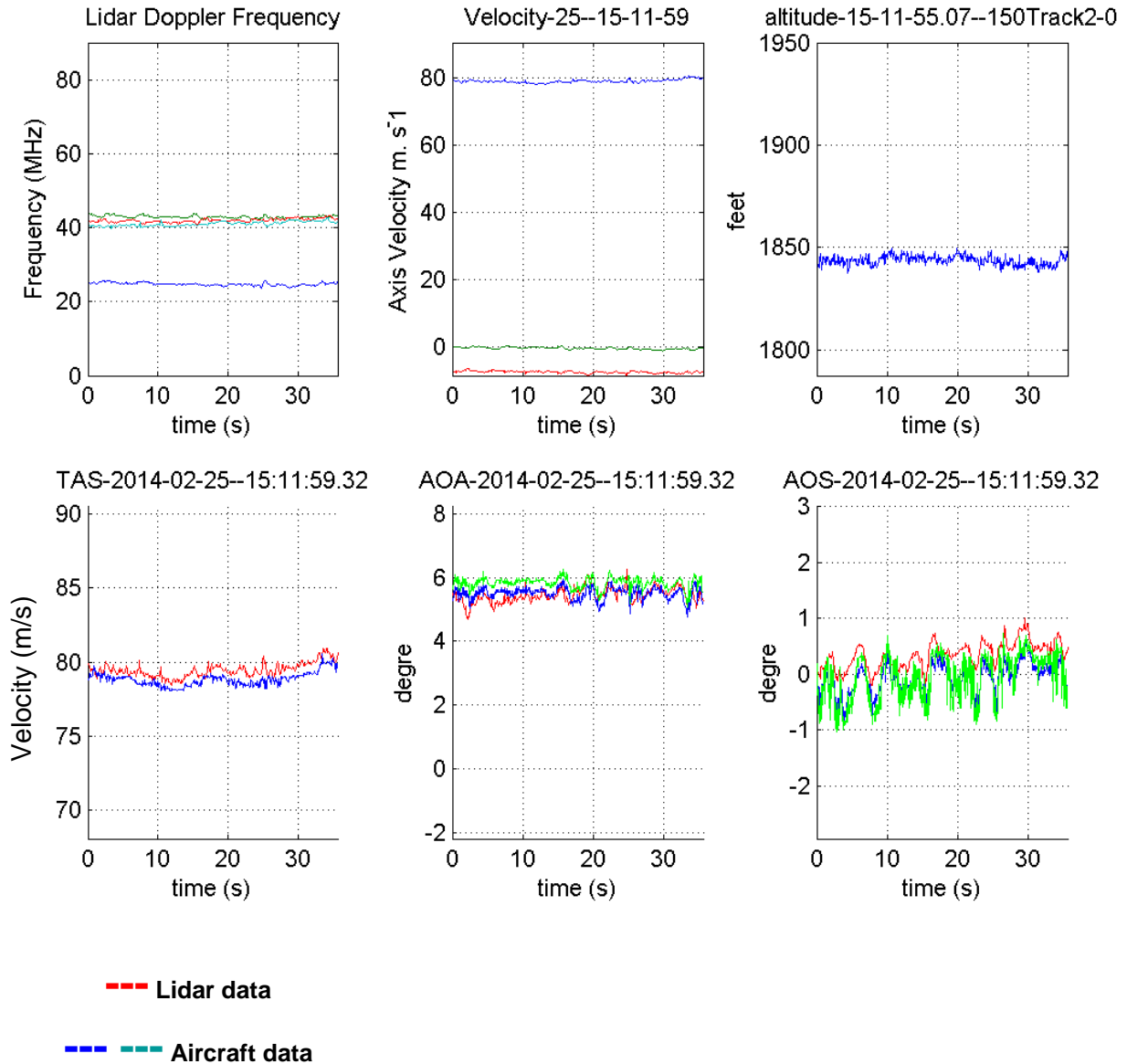


Figure 8: Multiple ground track for airspeed error.

The test (Figure 8) consists in 3 steady flights done at the same air speed (150 kts in this case), but with 3 different bearings.

Parameters are almost constants, as expected, with the exception of AOS having sub hertz oscillation of 1 degree in amplitude. This behavior will often be encountered in the next comparisons, but the effect was not perceptible inside the aircraft.

The agreement between both systems is within the requirements.

## Use of LIDAR in dynamic calibration

- LIDAR anemometer results in dynamic calibration: RollerCoaster for AOA - Pull up

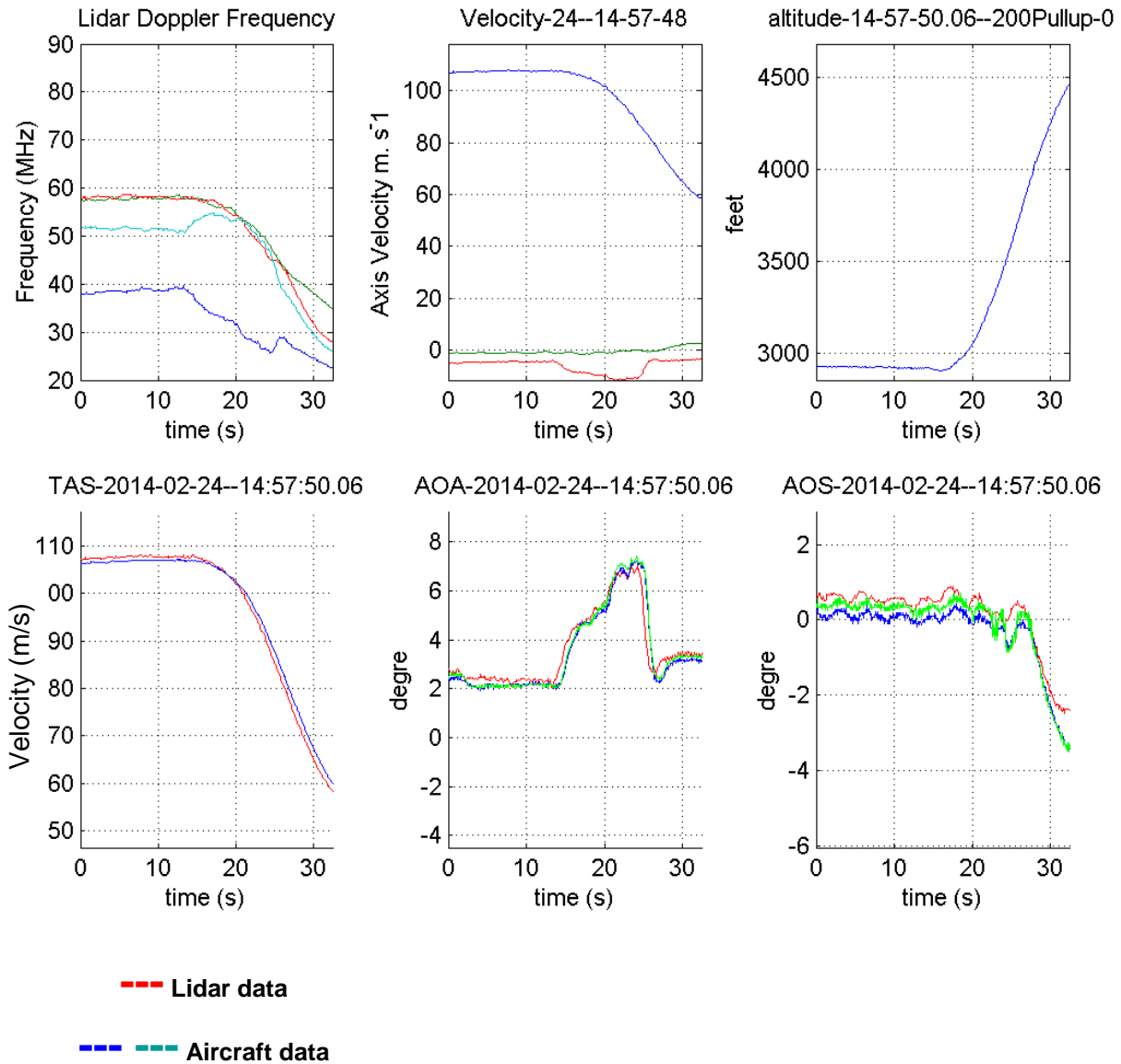


Figure 9: RollerCoaster for AOA – Pull up.

In this test (Figure 9), the aircraft performs a pull up maneuver at 2.5 g. The maneuver starts at 15s, and the AOA rises, and the pull up ends at 25s, and AOA decreases.

Despite being synchronized with GPS time, the LIDAR is almost 1s ahead of FTI. Again, the agreement between both systems is within the requirements.

➤ LIDAR anemometer results in dynamic calibration: Level Acceleration.

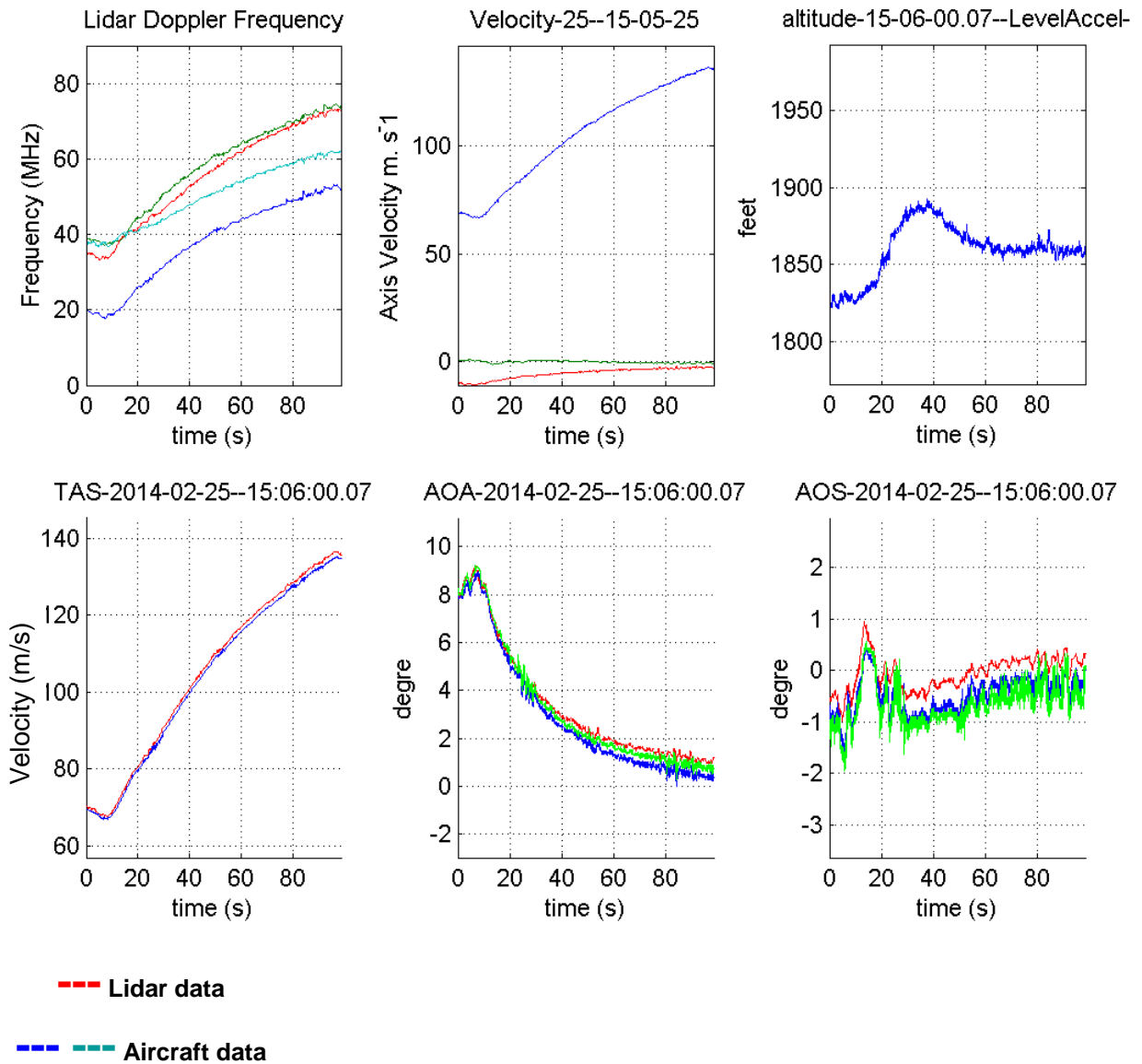


Figure 10: Level Acceleration.

The aircraft accelerates in straight line from 130 kts to 260 kts. The agreement between LIDAR and FTI is still within  $0.5^\circ$  for AOA/AOS and  $1 m \cdot s^{-1}$  for TAS, with a better agreement at high values of AOA (Figure 10).

➤ LIDAR anemometer results in dynamic calibration: Flat turn left for AOS .

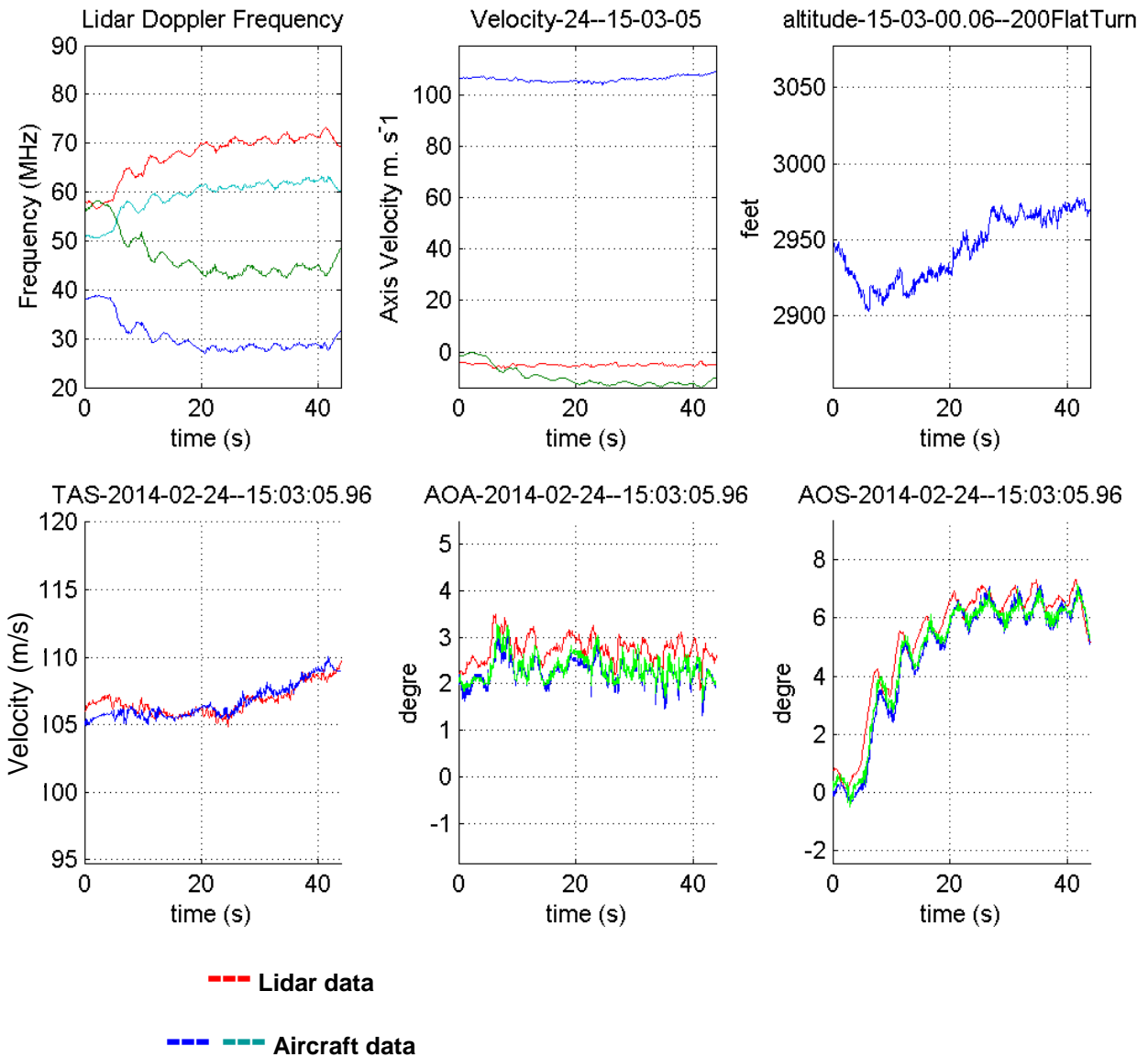


Figure 11: Flat turn left for AOS.

In this maneuver (Figure 11), the aircraft enters in a flat turn using its rudder, thus increasing AOS. The agreement between LIDAR and FTI is still within  $0.5^\circ$  for AOA/AOS and  $1 \text{ m}\cdot\text{s}^{-1}$  for TAS. The 1s advance of LIDAR over FTI is still visible.

### **3. Analysis**

An All-fiber 1.5  $\mu\text{m}$  CW coherent laser anemometer has been developed in the framework of the European project AIM2 and air qualified for calibration of Piaggio aircraft air data system.

Flight tests were performed successfully onboard the Piaggio P180. During 3 hours of flight tests, 40 LIDAR data sets have been recorded for comparison with aircraft Flight Test Instrument (FTI) data. For all recordings, Lidar air data have been graphically compared to the air data provided by the a/c Flight Test Instrumentation. This analysis has been done in the reference frame of the Lidar sensor head. Very good agreement on TAS, AOA and AOS variations were observed. A slight bias on AOA and AOS was observed but it remains below the  $0.5^\circ$  specification. Assuming perfect calibration of the FTI, the bias value is the result of two sources of error: 1- the precision of the mechanical adjustment of the Lidar sensor head with respect to the aircraft reference frame, 2- the uncorrected position of the Lidar sensor head reference frame with respect to the aircraft centre of rotation used for the data analysis. The latter should be compensated for in further data analysis.

It should also be mentioned that a lack of Lidar data was observed momentarily during flight tests over the sea, but due to the small number of flight tests conducted up to now, it is not possible to conclude on Lidar measurement availability. Further analysis and an extension of the flight campaign would be required in order to provide statistics on the Lidar data availability [9].

### **4. Conclusion**

From these results, we conclude that fiber Lidar technology has matured enough to provide a powerful technique for aircraft certification and in particular for onboard anemometry probes calibration (pitot, AOA, AOS). One main asset of the Lidar sensor is that it allows an absolute measurement of true air speed away from airframe aerodynamic perturbations and can significantly reduce the cost of certification procedures.

### **Acknowledgement**

Onera is grateful to Piaggio for its fruitful and efficient collaboration during AIM2 Lidar flight tests, and DLR supportive coordination throughout the project.

Onera also acknowledges the European Union for its financial support for AIM2 project (grant agreement n° 314237).

## REFERENCES

1. I. Mandle, "A laser anemometer reference for AIR data calibration", Aerospace and Electronics Conference, NAECON 1988., Proceedings of the IEEE 1988 National.
2. J.-P. Cariou, B. Augere, M. Valla, "Laser source requirements for coherent Lidars based on fiber technology", *Comptes Rendus Physique*, Tome7/Fascicule 2 (2006).
3. Scott M. Spuler, Dirk Richter, Michael P. Spowart, and Kathrin Rieken, "Optical fiber-based laser remote sensor for airborne measurement of wind velocity and turbulence", *Applied Optics/Vol. 50, No. 6 / 20* (February 2011).
4. H. Inokuchi, H. Tanaka, and T. Ando, "Development of a long range airborne Doppler Lidar", 27<sup>th</sup> International Congress of the Aeronautical Sciences (2010).
5. J.-P. Cariou, B. Augere, D. Goular, J.-P. Schlotterbeck, et X. Lacondamine, "All-fiber 1.5  $\mu\text{m}$  CW coherent laser anemometer DALHEC. Helicopter flight test analysis", 13th Coherent Laser Radar conference , Kamakura (2005).
6. B. Augere, D. Goular, M. Valla, C. Planchat, D. Fleury, "D5.5: Development of LIDAR for dynamic testing of AOA, AOS and static error correction", RT 1/18070 DOTA (March 2013).
7. B. Augere, D. Goular, M. Valla, C. Planchat, D. Fleury, "Description of the LIDAR sensor dedicated to AIM2 flight tests onboard P180 Piaggio aircraft", DOTA-AIM2-18070-RT-0034-1 (January 2013).
8. Takashi Fujii and Tetsuo Fukuchi, "Laser Remote Sensing", Chap 7.4, p508, Taylor&Francis Group Edition (2005).
9. V. Srivastava, J. Rothermel, A. D. Clarke, J. D. Spinhirne, R. T. Menzies, D. R. Cutten, M. A. Jarzembski, D. A. Bowdle, and E. W. McCaul, "Wavelength dependence of backscatter by use of aerosol microphysics and Lidar data sets: application to 2:1  $\mu\text{m}$  wavelength for space-based and airborne Lidars," *Appl. Opt.* 40, 4759–4769 (2001).